Available online at www.sciencedirect.com
SCIENCE DIRECT
Journal of Photochemistry and Photobiology A: Chemistry 179 (2006) 57–65
Journal of Photochemistry and Photobiology A:Chemistry
www.elsevier.com/locate/jphotochem

Photodeposition of CdSe using Se-TiO_2 suspensions as photocatalysts

Vi Nu Hoai Nguyen, Rose Amal *, Donia Beydoun

ARC Centre for Functional Nanomaterials, School of Chemical Engineering and Industrial Chemistry, UNSW, Sydney, NSW 2052, Australia

Received 19 December 2004; received in revised form 30 June 2005; accepted 12 July 2005
Available online 31 August 2005

Abstract

The photodeposition of cadmium selenide (CdSe) using Se-TiO_2 photocatalysts was studied at pH 3.5 and 7 in the presence of formic acid. The Se-TiO_2 photocatalysts were obtained by Se ion photoreduction using selenite (Se(IV)) and selenate (Se(VI)) as precursors. The formation of cadmium selenide was attributed to the reaction between cadmium ions and selenide ions (Se^{2-}) released from the Se deposited on TiO_2 particles under illumination. The release of the Se^{2-} ions from the Se–TiO_2 is believed to be the determining step for the formation of the CdSe particles, hence controlling their morphology as either rod-shaped or spherical. Metallic cadmium was also detected on the surface of TiO_2 particles as a product of the photocatalytic reduction at pH 7. Its formation was attributed to the photoreduction of cadmium by the photogenerated electrons in the TiO_2 and/or the Se semiconductors.

Keywords: Cadmium selenide; Photocatalytic reduction; Titanium dioxide; Mechanism; Morphology

1. Introduction

Cadmium selenide (CdSe) is an n-type semiconductor. Its bandgap energy was reported to be in the range from 1.65 to 1.8 eV [1–4]. CdSe was found to be suitable for various optoelectronic applications such as light-emitting diodes, laser diodes [5–8], catalysis [9], solar cells [10] and biological labelling [11]. The narrow bandgap CdSe has also been used for sensitising wide bandgap semiconductors such as titanium dioxide (E_g (TiO_2) = 3.2 eV) that can only be excited by 5% of UV light containing in the sunlight. The CdSe-sensitised TiO_2 has shown to improve the photoresponse in solar cells [12,13] and the efficiency in photocatalytic processes [14,15], compared to that of TiO_2 alone.

Sensitising TiO_2 with CdSe has been studied by a number of people, most of who have used the chemical deposition method [16–20]. Chenthramarakshan et al. [21] and Somasundaram et al. [15] suggested that selenium (Se)-modified TiO_2 obtained from photocatalytic reduction of selenite (Se(IV)) could be employed to produce CdSe–TiO_2 particles using the photocatalytic process. In those studies, two mechanisms for the formation of CdSe were proposed: either ionic or atomic. In the ionic pathway, CdSe was formed due to the reaction between cadmium ions and selenide ions released from the pre-deposited Se(0). The atomic pathway first involved the reduction of cadmium ions to the metallic form and then the reaction of the metal with deposited Se(0) due to the underpotential effect.

Photocatalytic processes involve irradiation of a semiconductor such as TiO_2 with energy greater than or equal to the band gap of the semiconductor. This promotes electrons from the valence band to the conduction band, generating photoexcited electrons (e^-) and holes (h^+). The photoexcited electrons and holes may diffuse to the surface of the semiconductor, followed by interfacial electron transfer to and from adsorbed acceptor and donor molecules. The holes are involved in the oxidation reactions, typically the mineralisation of organic substances present in the solution. Simultaneously, inorganic ions such as cadmium and selenium can be reduced to their elemental forms by the photogenerated electrons.

The TiO_2 photocatalytic reduction of selenium from its compounds (selenite (Se(IV) and selenate (Se(VI)) has been

* Corresponding author. Tel.: +61 2 9385 4361; fax: +61 2 9385 5966.
E-mail address: r.amal@unsw.edu.au (R. Amal).

1010-6030/$ – see front matter © 2005 Elsevier B.V. All rights reserved.
doi:10.1016/j.jphotochem.2005.07.012

extensively studied [22–28]. From such studies it has been found that selenium could be photoreduced to its elemental form and deposited onto the TiO_2 particles in the presence of formic acid as a hole scavenger.

From the work carried out on cadmium photocatalytic reduction using TiO_2 [29], we have found the conditions for this reaction are stricter than those required for selenium reduction. Cadmium was photoreduced only at pH 7 using formate ions as hole scavengers. The effective photoreduction of cadmium was attributed to the ability of cadmium and the formate ions to adsorb onto the TiO_2 particle surface, with the formate ions forming the highly reducing formate radicals.

It is known that electrical and optical properties of II–VI semiconductors such as CdSe closely depend on their size and shape [4,30–32]. The ability to control the morphology of semiconductor nanocrystals can provide an opportunity to test theories of quantum confinement [33,34], and produce samples with desirable optical characteristics for different applications [35,36]. To the best of our knowledge, no study has been carried out to investigate the CdSe morphology formed by the TiO_2 photocatalytic process. Therefore, the aim of this study is to clarify the mechanism of the photodeposition of CdSe employing Se-TiO_2 photocatalysts and hence gains a better understanding of the photocatalytic formation of CdSe particles and their morphology. In this report, we also studied effects of Se–TiO_2 formed from different selenium ion precursors (Se(IV) or Se(VI)) on the CdSe morphology. The optimum conditions reported previously for the photoreduction of selenium [25] and cadmium [29] were followed.

2. Experimental section

2.1. Chemicals

Cadmium perchlorate, sodium selenite, sodium selenate, formic acid, perchloric acid, sodium hydroxide and copper sulphate were all of reagent grade and used without further purification. All water used was Milli-Q deionised water. Degussa P25 TiO_2 was used as the photocatalyst.

2.2. Apparatus

The photocatalytic experiments were performed in a glass reactor as described in detail by Tan et al. [25]. It had a lid equipped with sampling ports. Oxygen was evacuated from the system by purging with nitrogen. The contents of the reactor were stirred throughout the experiment. A 1 L reaction solution was employed and illuminated by a 200 W Hg lamp, providing UV light of wavelength below 380 nm. The pH of the solution was controlled manually with $HClO_4$ and NaOH to maintain pH 3.5 for the preparation of Se–TiO_2 particles, and pH 3.5 or 7 for cadmium selenide photodeposition. It should be noted that as the reduction of Se(IV) and Se(VI) could result in the production of H_2Se, which is a toxic gas, the reactor system was connected to two scrubbers in series, containing $CuSO_4$ and NaOH solutions to capture the H_2Se gas.

2.3. Procedure

2.3.1. Preparation of Se–TiO_2 suspensions

The procedure for the photoreduction of selenium was described in more detail elsewhere [25]. In this study, a solution containing sodium selenite (or selenate), 300 ppm C formic acid and the TiO_2 photocatalyst (with a loading of 1.5 g/L) were equilibrated in the dark for 20 min at pH 3.5 and then the UV light was switched on. The illumination time was determined depending on the initial concentrations of Se ions and on whether selenite or selenate ions were used as the precursor. This was to reduce the maximum amount of Se ions and to make sure that the selenium remaining in the suspensions was the same if any left. Starting with 20-ppm selenite as precursor, 2 h of illumination were sufficient to complete the reaction. A 4-h illumination time was needed for an initial 40-ppm selenite and 20 ppm selenate concentration. Eight hours of illumination were needed for completing the reaction when starting with a 40-ppm selenate solution. The resulting Se–TiO_2 suspensions were then used directly for Cd photoremoval/reduction experiments (without washing or drying). Note that the characteristics of these Se–TiO_2 suspensions had been presented in our earlier publications [25,37].

2.3.2. Photodeposition of CdSe using Se–TiO_2 suspensions

These experiments involved introducing cadmium ions (as cadmium perchlorate) into the photoreactor directly after the photocatalytic reduction of selenium. Prior to irradiation, cadmium ions were equilibrated with the Se–TiO_2 suspensions for 30 min. Our previous study [28] found that with the addition of 300 ppm C formic acid a large amount (approximately 290 ppm C) still remained in the solution after the Se photoreduction. Hence, no additional organic hole scavenger was added into the system for the cadmium photoreaction. After the equilibration period, a suspension aliquot of 10 mL was collected and immediately filtered through a 0.22 μm syringe filter to remove the Se–TiO_2 particles. The filtrate was analysed for cadmium ions. This concentration was taken as the concentration of Cd in solution at the beginning of the photocatalytic reaction. The Hg lamp was then switched on. Aliquots of 10 mL were taken at interval times, filtered, stabilised in 2% HNO_3 and analysed for cadmium. The presence of selenium in the solution during cadmium photoremoval/reduction was also monitored. No selenium was detected in the solution following irradiation. In the absence of UV light illumination, no further removal of Cd was observed after the dark adsorption period.

2.4. Analysis

A Perkin-Elmer Optima 3000 ICP-OES Spectrometer was used for cadmium, selenium and copper analyses. Each

sample was analysed in triplicate. All analyses obtained had a relative standard deviation (R.S.D.) of less than 3%.

2.5. Characterisation studies

Methyl viologen was used as an indicator for metallic cadmium deposited on the surface of TiO_2. High resolution transmission electron microscopy (HRTEM) images were obtained using a Philips CM200. X-ray photoelectron spectroscopy (XPS) was performed on a VG ESCA LAB 220 I-XL model with the photon source of Al Kα to determine the oxidation states of cadmium and selenium. The binding energies were calibrated to the internal standard C 1s peak (285.00 eV). The zeta potential measurements on the Se–TiO_2 suspensions were obtained directly after the Se(IV) or Se(VI) photoreduction using ZetaPALS from Brookhaven Instrument Co. UV–vis reflectance measurements were carried out using a Varian Carry 5 UV–vis–NIR spectrometer employing $BaSO_4$ as reference. The absorbance spectra were obtained from the reflectance measurements using the Kubelka–Munk relationship.

3. Results and discussion

3.1. Study of cadmium adsorption on Se–TiO_2 particles

The results for the cadmium adsorption in the presence of formic acid using Se-modified TiO_2 as the photocatalyst at pH 3.5 and 7 are shown in Table 1. The adsorption of cadmium, using bare TiO_2 as the photocatalyst is also shown for comparison.

As can be seen from Table 1, in the presence of Se–TiO_2 suspension, no adsorption of cadmium ions was observed at pH 3.5 while at pH 7 a substantial amount of cadmium was adsorbed. The increase in cadmium concentration from 30 to 50 ppm increased the amount of cadmium adsorbed on the surface of the Se-TiO_2 catalysts, indicating that the adsorption equilibrium of cadmium ions had not been reached. With an initial concentration of cadmium at 30 ppm, the amount of cadmium adsorbed ranged from 15.1 to 16.9 mg/g catalyst for all the Se–TiO_2 suspensions while the initial concentration of 50 ppm Cd resulted in the adsorption of 19.4–21.3 mg Cd/g catalyst. This suggests that the amount of Se deposited on the TiO_2 particles and the types of precursors used had little effect on cadmium adsorption. This also indicates that the adsorption of cadmium was most likely due to the electrostatic attraction between the negatively charged Se–TiO_2 at pH 7 (Table 1) and the cation Cd^{2+}.

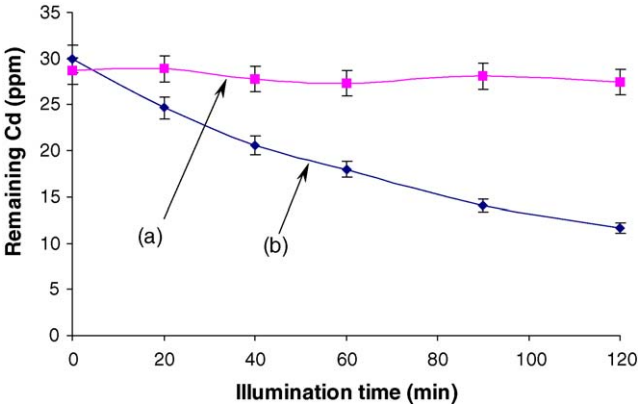

Fig. 1. Photoreduction/removal of cadmium using Se–TiO_2 suspension in the presence of formic acid. *Conditions*: The solution was illuminated after 30 min of dark adsorption. Initial Cd: 30 ppm; pH 3.5; catalysts: (a) bare TiO_2; (b) Se-TiO_2 suspension obtained using 20 ppm Se(IV).

3.2. Photoremoval/reduction of Cd ions using Se–TiO_2

Our earlier study on the photoreduction/removal of cadmium found that cadmium was not reduced/removed at pH lower than 7 [29]. In this study, the effectiveness of Cd removal at pH 3.5 was re-examined, this time using Se-TiO_2 suspensions as photocatalysts. The results of these photocatalytic reduction experiments using bare TiO_2 and Se-TiO_2 photocatalysts at pH 3.5 are compared in Fig. 1.

From Fig. 1, it can be seen that at pH 3.5, 2 h of illumination led to approximately 20 ppm of cadmium removal using the Se-TiO_2 photocatalyst compared to zero removal using

Table 1
Adsorption of cadmium on Se–TiO_2

Catalysts	Se(IV)[a]20[b]–TiO_2	Se(IV)[a]20[b]–TiO_2	Se(IV)[a]40[c]–TiO_2	Se(VI)[d]20[b]–TiO_2	Se(VI)[d]40[c]–TiO_2	Bare TiO_2
pH	3.5	7	7	7	7	7
Zeta potential (mV) (±2)	+9	−10	–	−12	–	−5
Cd30[e] adsorption (mg/g catalyst)	Negligible	16.9	15.5	15.6	15.1	14.9
Cd50[f] adsorption (mg/g catalyst)	–	19.4	20.1	20.6	21.3	18.8
R.S.D. (%)	3					

After Se photoreduction was completed the Se–TiO_2 suspensions were directly used for zeta potential measurements. Zeta potential for bare TiO_2 at pH 3.5 was measured to be +6 ± 2 mV.

[a] Selenite used as precursor.
[b] The initial precursor concentration of 20 ppm.
[c] The initial precursor concentration of 40 ppm.
[d] Selenate used as precursor.
[e] Initial concentrations of cadmium of 30 ppm.
[f] Initial concentrations of cadmium of 50 ppm.

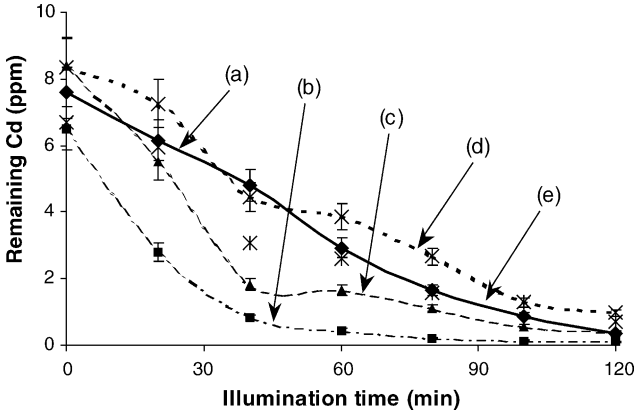

Fig. 2. Photoreduction/removal of cadmium using Se–TiO_2 suspension in the presence of formic acid. *Conditions*: The solution was illuminated after 30 min of dark adsorption. Initial Cd: 30 ppm; pH 7 for Cd removal; catalysts: (a) bare TiO_2; (b) and (c) Se-TiO_2 suspensions obtained using 20 and 40 ppm Se(IV); (d) and (e) Se-TiO_2 suspensions using 20 and 40 ppm Se(VI).

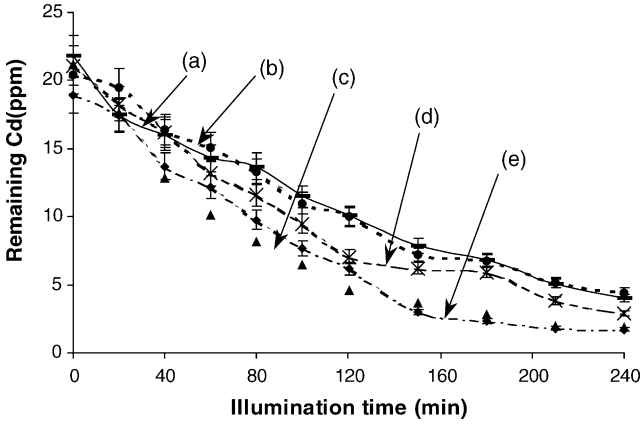

Fig. 3. Photoreduction/removal of cadmium using Se–TiO_2 suspension in the presence of formic acid. *Conditions*: The solution was illuminated after 30 min of dark adsorption. Initial Cd: 50 ppm; pH 7 for Cd removal; catalysts: (a) bare TiO_2; (b) and (c) Se-TiO_2 suspensions obtained using 20 and 40 ppm Se(IV); (d) and (e) Se-TiO_2 suspensions using 20 and 40 ppm Se(VI).

the bare TiO_2 photocatalyst. This indicates that the presence of selenium on the TiO_2 surface played an important role in the removal of cadmium ions upon illumination.

Our previous studies on Se(IV) and Se(VI) photoreduction at low pH [25–28] found that when Se(IV) and Se(VI) were almost exhausted from the solution, the deposited Se(0) was further photoreduced to Se^{2-}. It is therefore believed that when cadmium ions were introduced to this system and the pH remained at 3.5, upon further illumination cadmium ions reacted with the released Se^{2-} to produce CdSe according to reaction (1):

$$Cd^{2+} + Se^{2-} \xrightarrow{h\nu, Se-TiO_2} CdSe \quad (1)$$

The next set of experiments explored the photoreduction of Cd ions using Se–TiO_2 at pH 7. The results are presented in Fig. 2 for an initial Cd concentration of 30 ppm.

An increase of pH from 3.5 to 7 led to an enhanced photoreduction/removal of cadmium ions. After 2 h of illumination at pH 7, little cadmium (0.1 ppm Cd) ions were detected in the Se–TiO_2 suspension (line b, Fig. 2), compared with 11.4 ppm Cd remaining in the solution at pH 3.5 (line b, Fig. 1). The enhanced removal of Cd ions at pH 7 compared to that at pH 3.5 may be explained by the photoreduction of Cd to metallic cadmium at pH 7 [29] and the additional reaction between Cd^{2+} and released Se^{2-} to form CdSe (reaction (1)).

To verify the reaction of Cd^{2+} and the photogenerated Se^{2-} at pH 7, a separate experiment was carried out in which the pH of the suspension after Se photoreduction was increased from 3.5 to 7 with further illumination, in order to test for the formation of Se^{2-}. No cadmium was added in this case. From this experiment it was found that during illumination at pH 7, the orange pink colour of the Se–TiO_2 suspension faded from orange pink and became pinkish white. This suggests the removal of Se(0) from the surface of the TiO_2 particles as Se^{2-} ions.

At this point, illumination was stopped and the pH of the suspension was dropped back to 3.5 while nitrogen gas continued being purged into the reactor. This resulted in the formation of black particles in the $CuSO_4$ scrubber indicating the precipitation of CuSe. This verified that at pH 7 the Se(0) on the TiO_2 surface had been photoreduced to Se^{2-}, which in the presence of protons at pH 3.5, formed H_2Se gas. From this, it is therefore believed as stated earlier, that at pH 7 Cd^{2+} reacted with the released Se^{2-} to produce CdSe through reaction (1). This confirmed the ionic mechanistic formation of CdSe proposed earlier [15,21].

After 120 min of illumination the use of Se–TiO_2 obtained from the photoreduction of Se(IV) resulted in slightly better overall removal of cadmium at pH 7, compared to that using Se–TiO_2 from Se(VI) photoreduction (comparing line b–c with line d–e, Fig. 2). It is also observed that the use of Se(IV)–TiO_2 resulted in faster rate of cadmium removal, compared to bare TiO_2 and Se(VI)–TiO_2 (comparing line b–c with line a and d–e, Fig. 2). On the other hand, the removal of cadmium in the presence of bare TiO_2 and Se(VI)–TiO_2 were comparable. It is also noted that the increase in the Se loading from 20 to 40 ppm did not make much difference in the overall removal of cadmium. This might be due to that even at a loading of 20 ppm Se there was enough selenium to effectively react with 30 ppm Cd. As the adsorption equilibrium had not been reached when using 30 ppm Cd, further experiments were carried out at a higher initial Cd concentration of 50 ppm to try and further differentiate between the performances of the Se-TiO_2 photocatalysts. The results of these experiments are presented in Fig. 3.

When the Cd concentration was increased to 50 ppm, slightly faster rates of Cd removal compared to the blank TiO_2 were observed when using the Se–TiO_2 suspension obtained from 40 ppm Se(IV) and Se(VI) after 4 h of illumination. The Se–TiO_2 suspensions prepared using the 20 ppm Se(IV) and Se(VI) precursors has similar removal rates compared to the

bare TiO_2 photocatalysts (comparing lines b and d with line a, Fig. 3). This might be due to that in the presence of higher concentration of Cd (50 ppm), at least 40 ppm of Se was required to obtain significant enhancement of Cd removal.

In general, the presence of Se(0) deposits on TiO_2 (using Se(IV) and Se(VI) as the precursors) had little effect on the removal of cadmium, compared to that using bare TiO_2. It is therefore postulated that the removal of Cd from solution through Cd reduction by the photocatalytic process and the CdSe formation by the reaction of Cd^{2+} with Se^{2-} upon illumination are of comparable rates.

Cadmium was photoreduced by the electrons generated from TiO_2 photocatalyst in the presence of formate ions at pH 7 [29]. In addition, in this system the involvement of the Se photogenerated electrons in the reduction of cadmium to its metallic form cannot be ruled out. This is due to the fact that the Se conduction band (−1.65 V) is far below the redox potential of Cd^{2+}/Cd couple (−0.403 V). It is believed that the photoreduction of cadmium ions to metallic cadmium at pH 7 contributed to a higher removal of cadmium than that observed at pH 3.5.

It should be mentioned that in our study, formic acid was used as the organic additive. This was to scavenge the photogenerated holes by the photooxidation of formic acid. The photooxidation of formic acid can produce formate radicals which have a high reducing power (E^0 ($^{\bullet}COO^-/CO_2$) = −1.8 V). Hence, this radical could also be involved in the photoreduction reactions.

3.3. Characterisation of the photoreduction products

During selenium photoreduction, the colour of the suspension changed from milky white to orange pink, indicating the formation of Se(0). When cadmium was added and the suspension was illuminated, the orange pink colour became pinkish brown. The colour of the suspension is believed to be due to the presence Se(0), CdSe and metallic cadmium. The latter could be reoxidised when exposed to air to form CdO.

3.3.1. Detection of the presence of metallic cadmium

Methyl viologen was used to check the production of metallic cadmium. Methyl viologen was added while maintaining a nitrogen purge into the system to prevent the oxidation of Cd to CdO. This was done 24 h after the reaction had ceased in order to make sure that there were no more radical species in the system. During these 24 h the system was also kept under a nitrogen environment. The use of this method for the detection of metallic Cd has been discussed in detail in our previous publication [29]. In the presence of reactive metallic cadmium, methyl viologen, which is colourless indicator, becomes blue as it is reduced by the metallic cadmium. For the system in which the photoreduction/removal of cadmium was carried out at pH 3.5, the addition of methyl viologen did not bring about a colour change, indicating the absence of metallic cadmium and suggesting that the removal of cadmium under these conditions was purely due to selenium leading to the formation of CdSe. On the other hand, the addition of methyl viologen to the reaction suspension after cadmium photoreduction/removal using the Se-TiO_2 photocatalyst at pH 7 did lead to a colour change to blue, indicating that at pH 7 some of the cadmium ions were photoreduced to their metallic form.

3.3.2. X-ray photoelectron spectroscopy (XPS) studies

The product particles recovered from the photoreduction/removal of 30 and 50 ppm cadmium at pH 7 using Se–TiO_2 suspensions prepared from the photoreduction of 40 ppm Se(IV) and Se(VI) were subjected to XPS analysis. For comparison, XPS analysis was also carried out on the Se–TiO_2 particles and the powder obtained from 30 ppm Cd photoreduction/removal at pH 3.5 using Se–TiO_2 suspension prepared from 20 ppm Se(IV) precursor.

The Se–TiO_2 powder prepared using Se(IV) as precursor showed the binding energy of the Se(0) 3d state at 55.01 eV, which is within the literature values ranging from 54.64 to 55.7 eV [38]. In the powder obtained from the reaction at pH 3.5 two Se 3d peaks were observed, one at 54.17 eV and the other at a lower binding energy of 53.27 eV. A peak of Cd 3d with a centre at 404.48 eV was also present. Comparing these with the literature [3,21] suggested that the values at 53.27 for Se 3d and 404.48 eV for Cd 3d corresponded to Se $^3d_{5/2}$ and Cd $^3d_{5/2}$ in CdSe, respectively. The change in the binding energy of Se 3d was attributed to the transfer of charges from the Se atom to the Cd atom as Se is more electronegative than Cd [39]. The binding energy at 54.17 eV can be attributed to the Se(0) deposits remaining on TiO_2.

For the powders obtained from Cd removal at pH 7 using Se–TiO_2 suspensions, the high resolution XPS results showed two binding energy values of Cd $^3d_{5/2}$ with the centres at 405.58 and 404.61 eV, and two binding energy values of Se $^3d_{5/2}$ at 53.25 and 54.31 eV. Comparing these with the literature [38] suggested that the value of 404.61 eV corresponded to Cd $^3d_{5/2}$ binding energy in CdSe while the binding energy at 405.58 eV can be attributed to CdO. In addition, the energy binding values of Se at 53.25 and 54.31 eV can be attributed to Se $^3d_{5/2}$ in CdSe and Se(0), respectively. These results confirmed that upon illumination of Se–TiO_2 suspension at pH 7 in the presence of cadmium ions, CdSe was produced and a fraction of Se(0) was still present on TiO_2 surface. The XPS results also confirmed the presence of CdO in the recovered powders. The presence of CdO is believed to be due to the reoxidation of the reactive metallic cadmium, which also formed on the surface of TiO_2 at pH 7, upon exposure to air.

3.3.3. Charaterisation of optical properties

UV–vis reflectance analysis was carried out on various systems of interest and the measurements were then converted to absorbance spectra using Kubelka–Munk function. These UV absorbance spectra are presented in Figs. 4–6. Fig. 4 shows the absorbance spectra of pure TiO_2, pure CdSe powder and a mixture of CdSe and TiO_2 powders (10 wt.% CdSe). The CdSe powder was produced in-house by purging

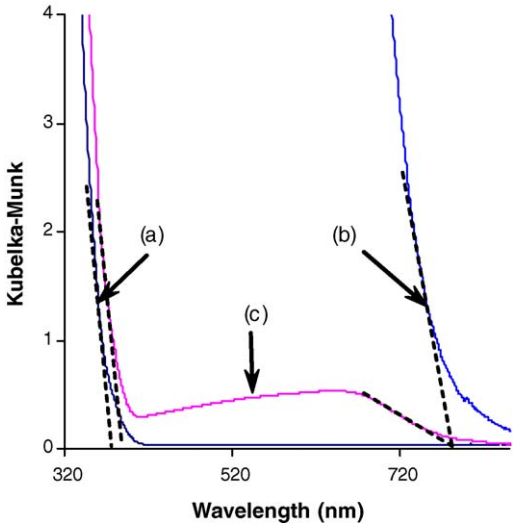

Fig. 4. Absorbance spectra of (a) pure TiO_2, (b) pure CdSe and (c) a physically mixture of 10 wt.% CdSe in TiO_2.

H_2Se gas into a $Cd(ClO_4)_2$ solution. Figs. 5 and 6 present the spectra for TiO_2 obtained from CdSe photodeposition experiments and the typical absorbance spectra of Se–TiO_2 powders obtained from the TiO_2 photocatalytic reduction of Se(IV) (line b, Fig. 5) and Se(VI) (line b, Fig. 6) for comparison. These spectra have two absorbance onsets at 400 and 680 nm wavelengths that can be attributed to the presence of TiO_2 particles and Se deposits, respectively [37].

As can be seen from Fig. 4, the absorbance spectrum of the mixture of CdSe and TiO_2 has two absorbance onsets at approximately 780 and 390 nm, corresponding to the presence of CdSe and TiO_2 particles, respectively. It is interesting to note that the onset for CdSe absorption was almost unchanged (at wavelength of 780 nm) while the TiO_2 typical absorbance onset at 380 nm was red shifted to the wavelength of 390 nm. From Figs. 5 and 6, when CdSe was photodeposited on TiO_2 by photocatalytic processes using Se-TiO_2 as catalysts, a further red shift to 400 nm, compared to that of pure TiO_2 absorbance onset at 380 nm, was observed in the spectra for all the resulting powders (lines c–f).

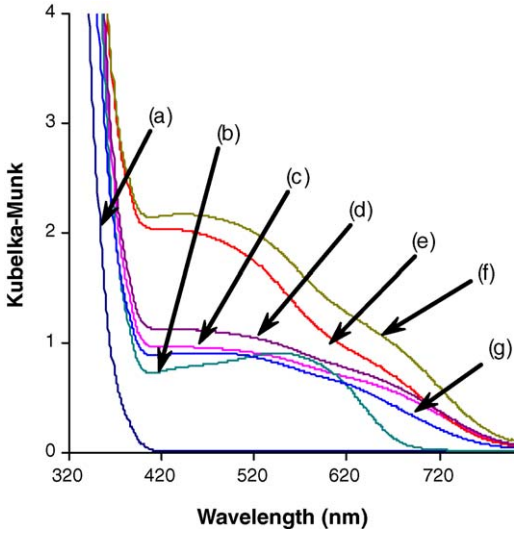

Fig. 5. Absorbance spectra of powders from Cd removal using Se-TiO_2 photocatalysts prepared from a selenite precursor: (a) pure TiO_2; (b) Se-TiO_2 obtained from photoreduction of 40 ppm Se(IV); (c) and (d) TiO_2 obtained from photoreduction of 30 and 50 ppm Cd at pH 7 using 20 ppm Se(IV) as precursor; (e) and (f) TiO_2 obtained from photoreduction of 30 and 50 ppm Cd at pH 7 using 40 ppm Se(IV) as precursor; (g) TiO_2 obtained from photoreduction of 30 ppm Cd at pH 3.5 using 20 ppm Se(IV) as precursor.

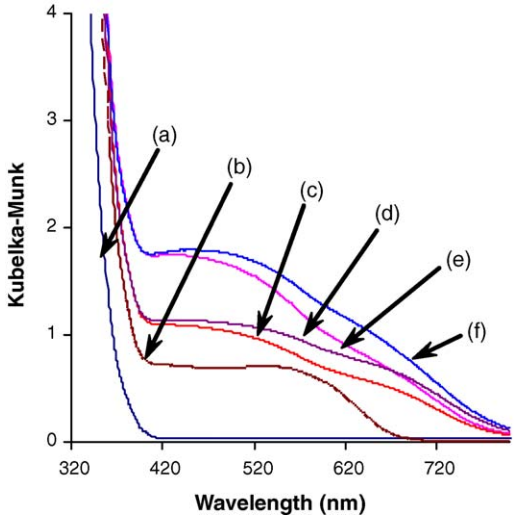

Fig. 6. Absorbance spectra of powders from Cd removal using Se-TiO_2 photocatalysts prepared from a selenate precursor: (a) pure TiO_2; (b) Se–TiO_2 obtained from photoreduction of 40 ppm Se(VI); (c) and (d) TiO_2 obtained from photoreduction of 30 and 50 ppm Cd using 20 ppm Se(VI) as precursor; (e) and (f) TiO_2 obtained from photoreduction of 30 and 50 ppm Cd using 40 ppm Se(VI) as precursor.

Theoretical and experimental work on II–VI core–shell particle system indicate that the bandgap energy of the system is influenced by the relative composition of the core–shell particle [40–42]. It is postulated here that the red shifts observed for CdSe–TiO_2 particles compared to pure TiO_2 in Figs. 5 and 6 are due to the hetero-junction between the core TiO_2 particles and the CdSe particles. Furthermore, the shift toward a longer wavelength that was observed for the CdSe-mixed TiO_2 powder in Fig. 4 may be indicative of electronic interactions even in physically mixed systems.

From Figs. 5 and 6, it can also be seen that all the spectra obtained for CdSe–TiO_2 particles have additional two shoulders starting at around 780 and 620 nm. Comparing with the spectrum of pure CdSe (line b, Fig. 4), the shoulder at 780 nm can be attributed to the presence of CdSe deposits. Hence, the UV–vis absorbance results confirm that CdSe was produced upon illumination of Se–TiO_2 suspensions in the presence of cadmium ions. Furthermore, compared to the spectra of Se–TiO_2 particles (line b, Figs. 5 and 6), the shoulder at 620 nm can be attributed to the presence of Se(0). This is also consistent with the results obtained from the XPS study.

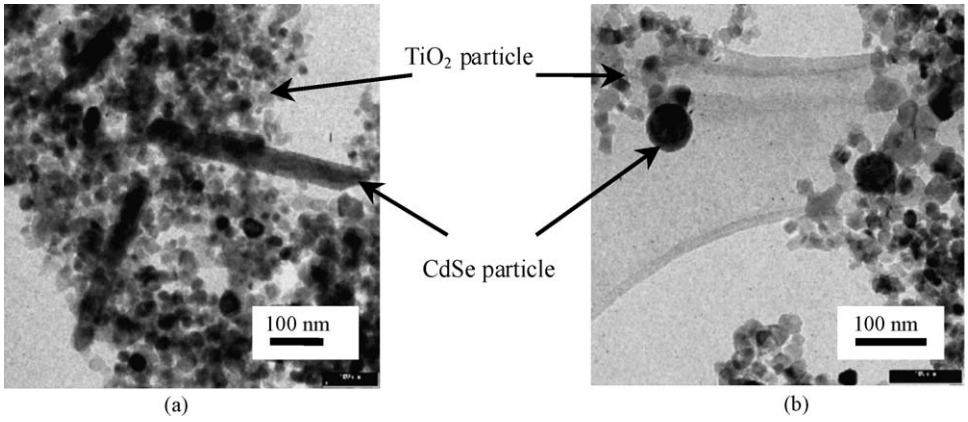

Fig. 7. TEM images of CdSe and TiO_2 particles after CdSe photodeposition experiments. Catalysts: (a) Se-TiO_2 obtained from photoreduction of 40 ppm Se(IV); (b) Se-TiO_2 obtained from photoreduction of 40 ppm Se(VI).

3.3.4. TEM characterisation of photodeposited CdSe using Se-TiO_2 as photocatalyst

Directly after the photodeposition of CdSe, an aliquot of the reaction suspension was transferred and placed on a carbon coated copper grid for TEM analysis. Images of the particles obtained from suspensions containing an initial 50 ppm Cd using Se-TiO_2 photocatalysts prepared from 40 ppm Se(IV) and Se(VI) precursors are shown in Fig. 7a and b, respectively.

The TEM analysis revealed that the photodeposition process had resulted in the formation of both rod-shaped and spherical-shaped CdSe particles. Interestingly, when using Se(IV)-TiO_2 as photocatalysts, the rod-shaped CdSe particles were the dominant morphology (Fig. 7a) while the use of Se(VI)-TiO_2 as the photocatalysts resulted in the dominance of the spherical CdSe particles (Fig. 7b). It should be emphasised that different morphological formation of CdSe from photocatalytic processes has not been reported before in the literature. High resolution TEM images (Fig. 8) showed that both rod-shaped and spherical CdSe particles consisted of nano-sized crystals. In addition, for both rod-shape and spherical CdSe particles [20,43], the electron diffraction pattern of these CdSe crystals (Fig. 8c) showed a typical lattice spacing of 3.51, 2.16 and 1.86 corresponding to the (1 1 1), (2 2 0) and (3 1 1) reflections of cubic structure. These indicate that both CdSe rods and spheres made up from nanocrystals of cubic structure. A postulation for the formation of different CdSe morphologies is put forward in the later section.

The morphology of a crystal depends on the growth rates of the different crystallographic faces. In fact, manipulation of growth kinetics has been used to control the shape of CdSe particles [44]. Peng et al. [44] showed that fast growth rates result in the formation of rod-shaped particles while nearly spherical particles are obtained when the overall growth rate is slow. Based on this, it is believed that a fast growth rate of CdSe in the Se(IV)–TiO_2 system resulted in the formation of rod-shaped CdSe particles while a slow growth rate in the Se(VI)–TiO_2 system brought about the formation of spherical CdSe particles.

3.4. An insight on the formation of different CdSe morphologies

As discussed earlier, this study confirmed that the ionic pathway of CdSe formation proposed by others [15,21] was the main mechanism in our reaction system. In this system, upon illumination of Se-TiO_2 photocatalysts the presence of cadmium ions resulted in the formation of CdSe via the reaction between Cd^{2+} and Se^{2-} at both pH 3.5 and 7 (reaction (1)). However, the question remained here as to how

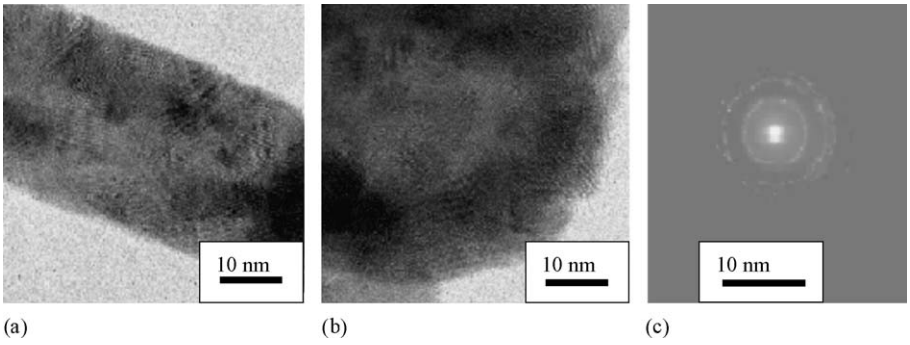

Fig. 8. High resolution TEM images showing the structure of the CdSe particles as being made up of many nano-sized crystals and their electron diffraction pattern: (a) rod-shape CdSe; (b) spherical CdSe; (c) electron diffraction pattern.

Se^{2-} was generated at pH 7, and whether the generation of Se^{2-} at both pH (3.5 and 7) followed the same mechanism. The generation of Se^{2-} at pH 3.5 has been discussed in detail in the study by Tan et al. [25], in which the reduction of Se(0) to Se^{2-} was attributed to the photogenerated electrons of the Se p-type semiconductor. Indeed, this could also be the case for Se^{2-} photogeneration at pH 7. The redox potential of couple Se/Se^{2-} in alkaline solution is −0.92 V (versus SHE), which is far below the conduction band of TiO_2 (−0.5 V versus SHE) at pH 7. Hence, the reduction of Se(0) by the TiO_2 photogenerated electrons is thermodynamically unfavourable. The conduction band of Se, on the other hand, is at −1.65 V, which has sufficient reducing power to reduce Se(0) to Se^{2-} at pH 7. Hence, at pH 7, it is postulated that the Se^{2-} was formed by the reduction of Se(0) by the photogenerated electrons in Se(0) deposits on TiO_2.

Furthermore, as discussed earlier, the TEM analysis revealed two morphologies of CdSe particles when using the Se–TiO_2 particles prepared from two selenium precursors (Se(IV) and Se(VI)). As cadmium ions were always available in the system, it could be expected that reaction (1) was independent of cadmium concentration and the release of Se as Se^{2-} was the rate determining step, hence controlling the morphology of the CdSe particles [44].

Our study on selenium photoreduction found that upon illumination of a TiO_2 suspension and using Se(IV) and Se(VI) as precursors the formation of both discrete Se particles and Se films was observed. However, the use of Se(VI) as precursor resulted in more discrete Se particles while Se(IV) precursor produced more evenly distribution of Se(0) deposits [25]. These different morphologies may have behaved differently and undergone different steps to produce selenide species.

The following sequence of reactions is believed to have occurred during CdSe formation. Upon illumination of the Se–TiO_2 suspensions, the Se(0) deposits were further photoreduced to Se^{2-} (reaction (2)), which then reacted with cadmium ions to form CdSe (reaction (3)). These two reactions are expected to be rather fast [45], resulting in the fast growth of CdSe particles. Hence, the result is the rod-shaped CdSe particles [44]:

$$Se^0 \xrightarrow{h\nu, TiO_2} Se^{2-} \quad (2)$$

$$Se^{2-} + Cd^{2+} \rightarrow CdSe \quad (3)$$

The generated Se^{2-} could also interact with Se(0) deposits to form polyselenide (reaction (4)) and be further photoreduced (reaction (5)) before reacting with Cd ions to form CdSe (reaction (6)) [46]:

$$Se^{2-} \xrightarrow{+xSe^0} (Se)_x^{2-} \quad (4)$$

$$Se_x^{2-} + 2(x-1)e^- \rightarrow xSe^{2-} \quad (5)$$

$$xSe^{2-} + xCd^{2+} \rightarrow xCdSe \quad (6)$$

The above described chain of reactions is believed to be responsible for the formation of cauliflower (three-dimension) structures of CdSe obtained from electrodeposition [46]. This may be compared with the spherical CdSe particles observed in this study (two-dimension, Figs. 7b and 8b).

It is noted that in addition to the dominant rod-shaped CdSe (obtained from photoreduction of Se(IV)–TiO_2) and spherical CdSe (from photoreduction of Se(VI)–TiO_2), a minor number of spherical and rod-shaped CdSe particles were also observed in these two systems, respectively. As the release of Se^{2-} governed the growth rate, hence the morphological formation of CdSe particles, it is of importance to control the generation of Se^{2-}. This may be achieved by controlling the formation of Se(0) deposits as either particles or films, which may be obtained by varying the initial concentrations of Se precursors in the photoreduction of Se ions. However, this is beyond the scope of the current study.

4. Conclusion

This study confirmed that upon illumination CdSe was photodeposited via the reaction between Cd^{2+} ions and Se^{2-} released from pre-deposited Se(0) on TiO_2. The current study further showed that the use of Se-TiO_2 photocatalysts obtained from the photoreduction of different selenium precursors (selenite and selenate) resulted in the dominance of different morphologies of the CdSe particles as either rod-shaped or spherical, respectively. This suggests a new approach to manipulate the properties of the CdSe during their formation, and hence control over electrical and optical properties of this semiconductor. Controlling size of these CdSe particles may be also worth to explore in the future.

Acknowledgements

This work was produced as part of the activities of the ARC Centre for Functional Nanomaterials funded by the Australian Research Council under the ARC Centres of Excellence Program. We thank the academic and technical staff from the School of Chemical Science, UNSW for their assistance with using the UV-Vis Cary 5 instrument, and the Electron Microscope Unit, UNSW for their assistance with the use of TEM. Vi N. H. Nguyen acknowledges AusAID for the scholarship provided for her Ph.D. study.

References

[1] P.V. Kamat, Photochemistry on nonreactive (semiconductor) surfaces, Chem. Rev. 93 (1993) 267–300.
[2] B. Su, K.L. Choy, Electrostatic assisted aerosol jet deposition of CdS CdSe and ZnS thin films, Thin Solid Films 361–362 (2000) 102–106.

[3] K.R. Murali, V. Swaminathan, D.C. Trivedi, Sol. Energy Mater. Sol. Cells 81 (2004) 113–118.
[4] K.R. Patil, D.V. Paranjape, S.D. Sathaye, A. Mitra, S.R. Padalkar, A.B. Mandale, Mater. Lett. 46 (2000) 81–85.
[5] V.L. Colvin, M.C. Schlamp, A.P. Alivosatos, Nature 370 (1994) 354–356.
[6] S.A. Empedocles, D.J. Norris, M.G. Bawendi, Phys. Rev. Lett. 77 (1996) 3873–3876.
[7] D.L. Klein, R. Roth, A.K.L. Lim, A.L. Alivisatos, P.L. McEuen, Nature 389 (1997) 699–701.
[8] C.C. Kim, S. Sinavathan, Phys. Rev. B 53 (1996) 1475–1484.
[9] T.S. Ahmadi, Z.L. Wang, T.C. Green, A. Henglein, M.A. El-Sayed, Science 272 (1996) 1924–1925.
[10] W. Huynh, X. Peng, A.P. Alivisatos, Adv. Mater. 11 (1999) 923–927.
[11] M. Bruchez Jr., M. Moronne, P. Gin, S. Weiss, A.P. Alivisatos, Science 281 (1998) 2013–2015.
[12] D. Liu, P.V. Kamat, J. Electroanal. Chem. 347 (1993) 451–456.
[13] R.N. Pandey, M. Misra, O.N. Srivastava, Inter. J. Hyd. Ener. 23 (1998) 861–865.
[14] S.C. Lo, C.F. Lin, C.H. Wu, P.H.J. Hsieh, Hazard. Mater. B114 (2004) 183–190.
[15] S. Somasundaram, C.R. Chenthamarakshan, N.R. de Tacconi, Y. Ming, K. Rajeshwar, Chem. Mater. 16 (2004) 3846–3852.
[16] J. Fang, J. Wu, X. Lu, Y. Shen, Z. Lu, Chem. Phys. Lett. 270 (1997) 145–151.
[17] J.H. Fang, X.M. Lu, X.F. Zhang, D.G. Fu, Z.H. Lu, Supramol. Sci. 5 (1998) 709–711.
[18] M.E. Ricon, A. Jimenez, A. Orihuela, G. Martinez, Sol. Energy Mater. Sol. Cells 70 (2001) 163–173.
[19] M.E. Ricon, O. Gomez-Daza, C. Corripio, A. Orihuela, Thin Solid Films 389 (2001) 91–98.
[20] Q. Shen, D. Arae, T. Toyoda, J. Photochem. Photobiol. A: Chem. 164 (2004) 75–80.
[21] C.R. Chenthamarakshan, Y. Ming, K. Rajeshwar, Chem. Mater. 12 (2000) 3538–3540.
[22] S. Sanuki, T. Kojima, K. Arai, S. Nagaoka, H. Majima, Metal. Mater. Trans. B 30B (1999) 15–20.
[23] S. Sanuki, K. Shako, S. Nagaoka, H. Majima, Mater. Trans. JIM 4 (2000) 799–805.
[24] E. Kikuchi, H.J. Sakamoto, Electrochem. Soc. 147 (12) (2000) 4589–4593.
[25] T.Y.T. Tan, M. Zaw, D. Beydoun, R. Amal, J. Nanopart. Res. 4 (2002) 541–552.
[26] T.T.Y. Tan, D. Beydoun, R. Amal, J. Mol. Catal. A: Chem. 202 (2003) 73–85.
[27] T.T.Y. Tan, D. Beydoun, R. Amal, J. Phys. Chem. B 107 (2003) 4296–4303.
[28] T.T.Y. Tan, D. Beydoun, R. Amal, J. Photochem, Photobiol. A: Chem. 159 (2003) 273–280.
[29] V.N.H. Nguyen, R. Amal, D. Beydoun, Chem. Eng. Sci. 58 (2003) 4429–4439.
[30] A.P. Alivisatos, Science 271 (1996) 933–937.
[31] C.M. Lieber, Solid State Commun. 107 (1998) 607–616.
[32] B. Pejova, I. Grozdanov, Mater. Lett. 58 (2004) 666–671.
[33] K. Leung, S. Pokrant, K.B. Whaley, Phys. Rev. 57 (1998) 12291–12301.
[34] A.L. Efros, M. Rosen, M. Kuno, M. Nirmal, D.J. Norris, M. Bawendi, Phys. Rev. 54 (1996) 4843–4856.
[35] X. Peng, J. Wickham, P. Alivisatos, J. Am. Chem. Soc. 120 (1998) 5343–5344.
[36] S.A. Empedocles, R. Neuhauser, M.G. Bawendi, Nature 399 (1999) 126–130.
[37] V.N.H. Nguyen, D. Beydoun, R. Amal, J. Photochem. Photobiol. A: Chem. 171 (2004) 117–124.
[38] NIST XPS Database, [online] 2001. Available: http://srdata.nist.gov/xps/Bind_e_spec_query.asp (September 5, 2003).
[39] M. Shenasa, S. Sainkar, D.J. Lichtman, Electron Spectrosc. Related Phenom. 40 (1986) 329–337.
[40] A.R. Kortan, R. Hull, R.L. Opila, M.G. Bawendi, M.L. Steigerwal, P.J. Carroll, L.E. Brus, J. Am. Chem. Soc. 112 (1990) 1327–1332.
[41] J.W. Haus, H.S. Shou, L. Honma, H. Komiyama, Phys. Rev. B 47 (1993) 1359–1365.
[42] S.H. Elder, F.M. Cot, Y. Su, S.M. Heald, A.M. Tyryshkin, M.K. Bowman, Y. Gao, A.G. Joly, M.L. Balmer, A.C. Kolwaite, K.A. Magrini, D.M. Blake, J. Am. Chem. Soc. 122 (2000) 5138–5146.
[43] S.N. Saragi, S.N. Sahu, Phisica E 23 (2004) 159–167.
[44] X. Peng, L. Manna, W. Yang, J. Wickham, E. Scher, A. Kadavanich, A.P. Alivisatos, Nature 404 (2000) 59–61.
[45] St. Kutzmutz, G. Lang, K.E. Heusler, Electrochim. Acta 47 (2001) 955–965.
[46] M. Tomkiewicz, I. Ling, W.S.J. Parsons, Electrochem. Soc.: Electrochem. Sci. Technol. 129 (1982) 2016–2022.